Journal of Rock Mechanics and Geotechnical Engineering 16 (2024) 1095–1105

Contents lists available at ScienceDirect

Journal of Rock Mechanics and Geotechnical Engineering

journal homepage: www.jrmge.cn

Technical Note

Limit state analysis of rigid retaining structures against seismically induced passive failure in heterogeneous soils

Jianfeng Zhou [a], Changbing Qin [b,c,d,*]

[a] College of Civil Engineering, Huaqiao University, Xiamen, 362021, China
[b] School of Civil Engineering, Chongqing University, Chongqing, 400045, China
[c] Key Laboratory of New Technology for Construction of Cities in Mountain Area, Chongqing University, Chongqing, 400045, China
[d] National Joint Engineering Research Center of Geohazards Prevention in the Reservoir Areas, Chongqing University, Chongqing, 400045, China

ARTICLE INFO

Article history:
Received 31 December 2022
Received in revised form
20 March 2023
Accepted 12 April 2023
Available online 4 June 2023

Keywords:
Retaining wall
Passive earth pressure
Earthquakes
Finite-element limit-analysis methods

ABSTRACT

Soils are not necessarily uniform and may present linearly varied or layered characteristics, for example the backfilled soils behind rigid retaining walls. In the presence of large lateral thrust imposed by arch bridge, passive soil failure is possible. A reliable prediction of passive earth pressure for the design of such wall is challenging in complicated soil strata, when adopting the conventional limit analysis method. In order to overcome the challenge for generating a kinematically admissible velocity field and a statically allowable stress field, finite element method is incorporated into limit analysis, forming finite-element upper-bound (FEUB) and finite-element lower-bound (FELB) methods. Pseudo-static, original and modified pseudo-dynamic approaches are adopted to represent seismic acceleration inputs. After generating feasible velocity and stress fields within discretized elements based on specific criteria, FEUB and FELB formulations of seismic passive earth pressure (coefficient K_P) can be derived from work rate balance equation and stress equilibrium. Resorting to an interior point algorithm, optimal upper and lower bound solutions are obtained. The proposed FEUB and FELB procedures are well validated by limit equilibrium as well as lower-bound and kinematic analyses. Parametric studies are carried out to investigate the effects of influential factors on seismic K_P. Notably, true solution of K_P is well estimated based on less than 5% difference between FEUB and FELB solutions under such complex scenarios.

1. Introduction

There are some conditions in practice where lateral pressures are generated to push soils. When a retaining wall experiences certain displacements to reach a limit equilibrium state, such lateral pressure corresponds to passive earth pressure beyond which soils would undergo passive failure. Comparatively, a much larger displacement is required for a retaining wall to reach its passive limit state, in contrast to active case. Nonetheless, such passive failure is also possible under large lateral pressures, for example, in the abutment of arch bridges. Apart from physical modelling, limit analysis is capable of providing rigorous upper and lower bounds to passive earth pressure analysis, and due to its efficacy, it is selected as the principal method used in this study, aiming to obtain the true solution at limit state.

Within the framework of plasticity theory, limit analysis consists of lower- and upper-bound theorems based on which true solution for the problem of interest can be well limited to a range of lower- and upper-bound solutions. It is worthwhile pointing out that it is challenging to perform a complete limit analysis due to the construction of a kinematically admissible velocity field and a statically allowable stress field, particularly in non-uniform soils. For simplification, preliminary studies were principally performed for homogeneous and isotropic soils (Chen, 1975; Chen and Liu, 1990), where linear Mohr-Coulomb (MC) criterion was adopted for calculating static and seismic passive earth pressures. Thereafter, some researchers (e.g. Soubra, 2000; Liu et al., 2018; Yang and Li, 2018; Li and Yang, 2019a, 2019b; Li et al., 2020) computed passive and active earth pressures acting on rigid retaining walls, from the perspective of upper bound theorem. In contrast, a lower bound analysis was carried out for evaluation of passive earth pressure in a homogeneous soil (Lancellotta, 2007). In order to account for non-

* Corresponding author. School of Civil Engineering, Chongqing University, Chongqing, 400045, China.
E-mail address: changbingqin@u.nus.edu (C. Qin).
Peer review under responsibility of Institute of Rock and Soil Mechanics, Chinese Academy of Sciences.

https://doi.org/10.1016/j.jrmge.2023.04.009

uniform soils, some techniques are necessitated for this specific purpose. For example, Qin and Chian (2020) proposed a discretization-based kinematic analysis procedure and combined the merits of discretization technique and upper-bound analysis to investigate pseudo-static and pseudo-dynamic passive earth pressures, in considerations of non-uniform soils. Definitely, finite-element upper-bound (FEUB) analysis is capable of considering almost all scenarios including non-uniform soil parameters, in the analysis of passive earth pressures. Note that in the study of Shiau et al. (2008), however, such powerful method was applied to evaluate passive earth pressures, merely accounting for uniform and cohesionless soils, without providing lower bound solutions. In contrast, a finite-element lower-bound (FELB) analysis was only performed in Fathipour et al. (2020, 2021) to evaluate lateral earth pressures by virtue of second-order cone programming. In the above literature, FEUB and FELB procedures were separately applied to assess passive earth pressures specific to limited scenarios, which is not the case in slope stability analysis where both upper- and lower-bound solutions were calculated (Oberhollenzer et al., 2018; Ukritchon and Keawsawasvong, 2018; Qin and Zhou, 2023; Zhou and Qin, 2023). Therefore, in order to estimate the true solution of seismic passive earth pressure, FEUB and FELB procedures are adopted and developed, which is the motivation of this study.

It is acknowledged that earthquake is a major trigger for engineering failure, including for retaining walls. Selection of earthquake inputs is imperative for accurate prediction of lateral earth pressures. Apart from the commonly used pseudo-static approach, pseudo-dynamic approach is mainly adopted in this study. Such approach provides a compromise between accurate but complex acceleration time-history and simple but approximate pseudo-static approach. The original pseudo-dynamic approach was proposed by Steedman and Zeng (1990), in order to represent a linearly varied horizontal acceleration when shear wave propagates along a retaining wall. This aids to mimic tempo-spatial earthquake effects. Thereafter, some authors adopted such approach to further estimate passive earth pressures, by means of limit equilibrium only (e.g. Choudhury and Nimbalkar, 2005; Nimbalkar and Choudhury, 2007). Note that, however, violation of zero stress boundary conditions at the ground surface exists in the original pseudo-dynamic approach. The modified pseudo-dynamic approach was accordingly developed to incorporate the spectral characteristics of site response analysis, so as to overcome such main drawback. The modified approach can also account for soil damping properties and nonlinearly varied acceleration with depth. It was then applied to investigate lateral earth pressures with limit equilibrium (Rajesh and Choudhury, 2017; Srikar and Mittal, 2020), method of stress characteristics (Santhoshkumar and Ghosh, 2020), as well as discretization-based upper bound analysis (Qin and Chian, 2020) and FELB analysis (Fathipour et al., 2020, 2021). Based on the above studies, true solution of passive earth pressure is still difficult to be estimated.

In this study, the core work is to develop dynamic FEUB and FELB procedures for the assessment of seismic passive earth pressure of backfilling soils on a rigid retaining wall, incorporating the modified pseudo-dynamic approach. Meanwhile, a linear variation in soil cohesion and friction angle is also incorporated in the procedures to encompass wider scenarios. Rigorous lower- and upper-bound solutions are calculated under complicated conditions, and based on which true solution of passive earth pressure is to be better estimated. Effects of influential factors on FEUB and FELB solutions and critical failure mechanisms are investigated to show its implication on the design of a retaining wall in earthquake-prone regions.

2. Problem description

This study is to investigate passive earth pressures of backfilling soils acting on a rigid retaining wall. Such wall is characterized by height H, and an inclination angle of λ, as illustrated in Fig. 1. When wall friction is considered, passive earth pressures are inclined at an angle of δ_w (wall friction angle) with respect to the outward-drawn normal direction of the wall. In this study, a linearly increased MC soil strength profile is considered, with soil cohesion (c_h) and friction angle (φ_h) at ground surface linearly increased to c_0 and φ_0 at wall base level. Note that boundary conditions must be satisfied, including zero velocity on vertical side boundaries and model bottom in FEUB analyses, and zero stress on ground surface in the absence of surface surcharge in FELB analyses. It is worthwhile highlighting that along wall back, unknown normal and shear stresses induced by passive earth pressures are exerted on backfilling soils in FELB analyses so as to meet stress equilibrium conditions at such boundary. In order to avoid boundary effects, a relatively large model is established.

3. Methodologies

3.1. Pseudo-dynamic earthquake methods

In the presence of an earthquake, a proper manner to characterize earthquake inputs directly affects the accuracy of lateral earth pressures. For comparison, the simplified pseudo-static approach (P-s), original pseudo-dynamic approach (P-d), and modified pseudo-dynamic approach (MP-d) are considered. In the P-s analysis, the horizontal and vertical seismic forces (accelerations) keep constant, to provide a quick estimate (Qin and Chian, 2020). Specific introduction of the P-d approach can be found in Qin and Chian (2018, 2019) where the magnitude of seismic accelerations varies linearly with depth by virtue of a constant amplification factor f, and the initial phase difference between horizontal and vertical accelerations is considered as zero in this study. The MP-d approach provides another way to consider earthquake inputs from the perspective of seismic response of soil displacement. By means of double differential of soil displacement, horizontal and vertical seismic accelerations are derived, satisfying the equation of motion of stress waves and boundary conditions. For discussion, the expressions of horizontal and vertical seismic accelerations ($a_h(t,y)$ and $a_v(t,y)$) at time t and position y are shown as below:

$$a_h(t,y) = \frac{k_h g}{C_S^2 + S_S^2} \cdot [(C_S C_{SZ} + S_S S_{SZ})\cos(\varpi t) + (S_S C_{SZ} - C_S S_{SZ})\sin(\varpi t)] \quad (1)$$

$$a_v(t,y) = \frac{k_v g}{C_P^2 + S_P^2} \cdot [(C_P C_{PZ} + S_P S_{PZ})\cos(\varpi t) + (S_P C_{PZ} - C_P S_{PZ})\sin(\varpi t)] \quad (2)$$

where k_h is the seismic horizontal coefficient at wall base, k_v is the seismic vertical coefficient at wall base, g is the gravitational acceleration, ϖ is the angular velocity (period $T = 2\pi/\varpi$). C_S, C_{SZ}, S_S, S_{SZ}, C_P, C_{PZ}, S_P, S_{PZ} are intermediate parameters expressed by the height of retaining wall H, position y, shear (primary) wave velocity V_S (V_P) and soil damping ratio ξ, which can be found in published literature (Pain et al., 2017; Rajesh and Choudhury, 2017).

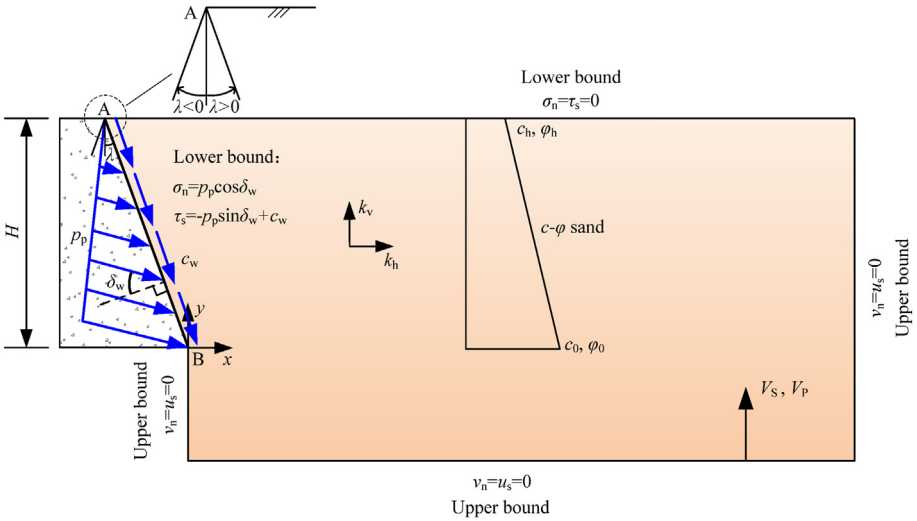

Fig. 1. Schematic of seismic passive earth pressure problem.

3.2. Finite-element lower-bound method

The lower-bound theorem demonstrates that geotechnical structures subject to traction force $\boldsymbol{T}_i$ and body force $\boldsymbol{X}_i$ would not fail, if a stress field $\boldsymbol{\sigma}_{ij}$ could be found, which is in equilibrium with forces $\boldsymbol{T}_i$ and $\boldsymbol{X}_i$ and also does not violate yield criterion. It is noted that in a lower bound analysis, equilibrium and yielding conditions are considered. A statically allowable stress field is therefore necessitated to derive lower-bound solutions.

The challenge of performing a lower-bound analysis lies in generating a statically allowable stress field, which inhibits the widespread use of such method to a great extent. Resorting to finite element method, the whole domain of interest is discretized into three-nodded triangular elements. Based on this, the stress field is to be generated by following the conditions: (i) stress equilibrium within each element, (ii) continuity of normal and shear stresses at the interface of two adjacent elements, (iii) stress boundary conditions, and (iv) no violation of MC yield criterion. Specifically, the above conditions are represented by stress components which are a linear combination of nodal stresses.

Based on the generated stress field, the traction force can be selected as the objective function of a lower-bound analysis, which is further transformed to a linear programming problem. Since this study aims to compute passive force P_p on a rigid retaining wall, it is chosen as the objective function and is expressed by integrating passive earth pressure P_p:

$$P_p = \int_s p_p \mathrm{d}s \tag{3}$$

where s is the portion of the boundary where P_p is applied.

In a lower-bound analysis, it is of interest to seek the highest lower-bound solution. Equivalently, optimization of passive force P_p is transformed to seek the maximal value of pressure p_p. When a dynamic analysis of passive earth pressures is investigated, time t is discretized into time increments, and an optimal $p_p(t)$ value is sought in each optimization. During earthquake period, a series of $p_p(t)$ values are obtained and the minimal one leading to failure of a retaining wall is deemed as the most dangerous. Accordingly, the linear programming model for dynamic passive earth pressure is

$$\underset{t,t\in[t_{\mathrm{start}},t_{\mathrm{end}}]}{\text{minimize}}\left\{\underset{\boldsymbol{X}}{\text{maximize}}\left[p_p(t)\right]\right\}\text{s.t.}\quad\begin{cases}\boldsymbol{A}_1\boldsymbol{X}=\boldsymbol{B}_1\\ \boldsymbol{A}_2\boldsymbol{X}=\boldsymbol{0}\\ \boldsymbol{A}_3\boldsymbol{X}=\boldsymbol{B}_3\\ \boldsymbol{A}_4\boldsymbol{X}\le\boldsymbol{B}_4\end{cases} \tag{4}$$

where $\boldsymbol{X}=\left[\sigma_{x1}\ \ \sigma_{y1}\ \ \tau_{xy1}\ \ \sigma_{x2}\ \ \sigma_{y2}\ \ \tau_{xy2}\ \ \cdots\ \ \sigma_{xnp}\ \ \sigma_{ynp}\ \ \tau_{xynp}\right]^{\mathrm{T}}$ is the vector of unknown stress components for a total of np nodes; $\boldsymbol{A}_1,\boldsymbol{B}_1,\boldsymbol{A}_2,\boldsymbol{A}_3,\boldsymbol{B}_3,\boldsymbol{A}_4,\boldsymbol{B}_4$ are the matrices of constraint coefficients which are respectively assembled from matrices $\boldsymbol{A}_1^{\mathrm{e}}$, $\boldsymbol{B}_1^{\mathrm{e}}$, $\boldsymbol{A}_2^{\mathrm{d}}$, $\boldsymbol{A}_3^{\mathrm{b}}$, $\boldsymbol{B}_3^{\mathrm{b}}$, $\boldsymbol{A}_4^{\mathrm{i}}$ and $\boldsymbol{B}_4^{\mathrm{i}}$, based on elementary analyses. Specific expressions of these parameters can also be found in the study of Qin and Zhou (2023).

Eq. (4) is optimized by an interior point algorithm implemented into MATLAB, so as to find out optimal passive earth pressures. Afterwards, the passive force is obtained through integral calculations. As for retaining wall problems, it is of much interest to present results in terms of dimensionless coefficients, for example passive earth pressure coefficient K_p in this study. Based on the assumption of a linear distribution of passive earth pressures along the wall, K_p is expressed as

$$K_p = \frac{2\int_s p_p \mathrm{d}s}{\gamma\left(\frac{H}{\cos\lambda}\right)^2} \tag{5}$$

where γ is the unit weight of backfilling soils.

3.3. Finite-element upper-bound method

The upper-bound theorem indicates that failure of geotechnical structures would occur or be imminent if applied external forces are no less than the load computed from the equilibrium of external and internal rates of work within a kinematically admissible velocity field. It is worth pointing out that in an upper-bound analysis, focus is placed on failure mechanism and energy dissipation (work rates) calculations, without considering equilibrium conditions of stress distribution. Prior to calculation of external and internal rates of work, generation of a kinematically admissible velocity field is a prerequisite.

Analogous to FELB analyses, the model is discretized to linear three-nodded triangular elements. In such a manner, the velocity variable in a velocity field can be expressed by a linear function of horizontal (u) and vertical (v) nodal velocities. In order to overcome the challenge in an upper-bound analysis, i.e. generation of a kinematically admissible velocity field, it shoud satisfy: (i) associative flow rule within each element, (ii) velocity discontinuities conditions, and (iii) velocity boundary conditions. By virtue of nodal velocities, the mathematical model of a kinematically admissible velocity field gives

$$\begin{cases} \boldsymbol{A}_{11}\boldsymbol{X}_1 - \boldsymbol{A}_{12}\boldsymbol{X}_2 = \boldsymbol{0} \\ \boldsymbol{A}_{21}\boldsymbol{X}_1 - \boldsymbol{A}_{23}\boldsymbol{X}_3 = \boldsymbol{0} \\ \boldsymbol{A}_{31}\boldsymbol{X}_1 = \boldsymbol{B}_{31} \end{cases} \tag{6}$$

where $\boldsymbol{X}_1 = [u_1 \quad v_1 \quad u_2 \quad v_2 \quad \cdots \quad u_{np} \quad v_{np}]^{\mathrm{T}}$ is the vector of nodal velocities for a total of np nodes; $\boldsymbol{X}_2 = [\dot{\lambda}_{11} \quad \dot{\lambda}_{12} \quad \cdots \quad \dot{\lambda}_{1p} \quad \dot{\lambda}_{21} \quad \dot{\lambda}_{22} \quad \cdots \quad \dot{\lambda}_{2p} \quad \cdots \quad \dot{\lambda}_{ne1} \quad \dot{\lambda}_{ne2} \quad \cdots \quad \dot{\lambda}_{nep}]^{\mathrm{T}}$ is the vector of plastic multiplier rates for ne elements in which MC yield criterion is linearized with a p-polygon; $\boldsymbol{X}_3 = [\dot{\xi}_{11} \quad \dot{\xi}_{12} \quad \dot{\xi}_{13} \quad \dot{\xi}_{14} \quad \dot{\xi}_{21} \quad \dot{\xi}_{22} \quad \dot{\xi}_{23} \quad \dot{\xi}_{24} \quad \cdots \quad \dot{\xi}_{nd1} \quad \dot{\xi}_{nd2} \quad \dot{\xi}_{nd3} \quad \dot{\xi}_{nd4}]^{\mathrm{T}}$ is the vector of plastic discontinuity multipliers for nd velocity discontinuities; $\boldsymbol{A}_{11}, \boldsymbol{A}_{12}, \boldsymbol{A}_{21}, \boldsymbol{A}_{23}, \boldsymbol{A}_{31}, \boldsymbol{B}_{31}$ are the matrices of constraint coefficients assembled from $\boldsymbol{A}^{\mathrm{e}}_{11}, \boldsymbol{A}^{\mathrm{e}}_{12}, \boldsymbol{A}^{\mathrm{d}}_{21}, \boldsymbol{A}^{\mathrm{d}}_{23}, \boldsymbol{A}^{\mathrm{b}}_{31}, \boldsymbol{B}^{\mathrm{b}}_{31}$, respectively. The expressions of these parameters can be found in Zhou and Qin (2020, 2022).

After having generated a velocity field based on Eq. (6), the next step is to express rates of work produced by internal and external forces in an upper bound analysis. Hereof, internal energy dissipation consists of two parts: W_{in1} within elements due to continuous deformation and W_{in2} on velocity discontinuities owing to plastic shearing:

$$W_{\mathrm{in1}} + W_{\mathrm{in2}} = \iint_A (\dot{\varepsilon}_x\sigma_x + \dot{\varepsilon}_y\sigma_y + \dot{\gamma}_x\tau_{xy})\mathrm{d}A + \int_0^l c(\dot{\xi}_{\mathrm{a}} + \dot{\xi}_{\mathrm{b}})\mathrm{d}l \tag{7}$$

where $\sigma_x, \sigma_y, \tau_{xy}$ are the planar stress components of a point within an element; $\dot{\varepsilon}_x, \dot{\varepsilon}_y, \dot{\gamma}_{xy}$ are the plastic strain rates; $\dot{\xi}_{\mathrm{a}}, \dot{\xi}_{\mathrm{b}}$ are nonnegative plastic discontinuity multiplier; A is the area of the model of interest; and l is the length of velocity discontinuities.

Applied external forces include body and extraction forces. When an earthquake is considered, seismic loading is usually regarded as body forces. The external rates of work by soil weight (W_{ex1}) and seismic forces (W_{ex3}) are therefore expressed as

$$W_{\mathrm{ex1}} + W_{\mathrm{ex3}} = \left[1 - \frac{a_{\mathrm{v}}(t,y)}{g}\right]\gamma\int_A v\mathrm{d}A + \frac{a_{\mathrm{h}}(t,y)}{g}\gamma\int_A u\mathrm{d}A \tag{8}$$

As for traction force, it consists of wall cohesion and passive force acting on potential failure block. The rates of passive earth pressure (W_{ex2}) and that of cohesive force (W_{ex4}) are written as

$$W_{\mathrm{ex2}} = \int_s \left[p_{\mathrm{p}}\sin(\delta_{\mathrm{w}} - \lambda)v + p_{\mathrm{p}}\cos(\delta_{\mathrm{w}} - \lambda)u\right]\mathrm{d}s \tag{9}$$

$$W_{\mathrm{ex4}} = \int_s (c_{\mathrm{w}}v\cos\lambda + c_{\mathrm{w}}u\sin\lambda)\mathrm{d}s \tag{10}$$

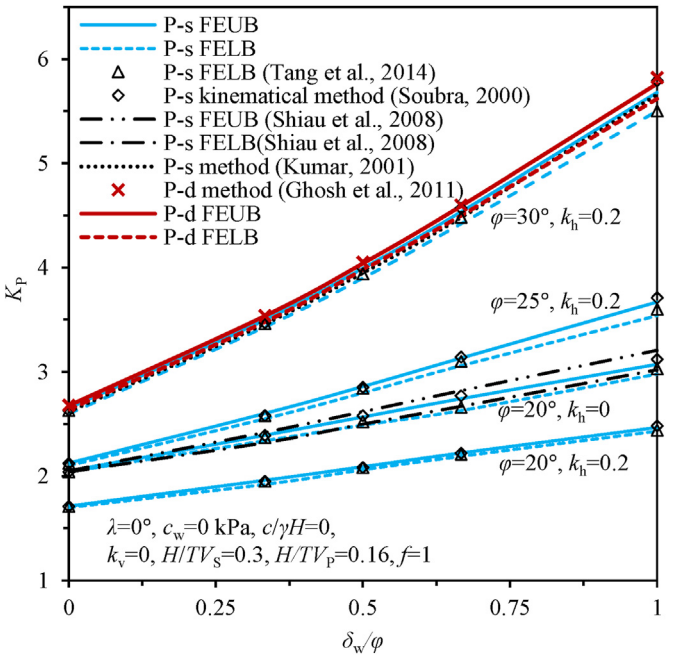

Fig. 2. Comparison of P-s and P-d solutions of K_{P} from different approaches.

where c_{w} is the wall cohesion, s is the length of wall back where p_{p} and c_{w} are applied.

Based on work rate balance equation, the upper bound formulation of passive earth pressure is

$$p_{\mathrm{p}} = \frac{W_{\mathrm{in1}} + W_{\mathrm{in2}} - W_{\mathrm{ex1}} - W_{\mathrm{ex3}} - W_{\mathrm{ex4}}}{\int_s \sin(\delta_{\mathrm{w}} - \lambda)v + \cos(\delta_{\mathrm{w}} - \lambda)u\mathrm{d}s} \tag{11}$$

For optimization, the nonlinear objective function of passive earth pressure is transformed to a linear programming model subjected to $\int_s \sin(\delta_{\mathrm{w}} - \lambda)v + \cos(\delta_{\mathrm{w}} - \lambda)u\mathrm{d}s = 1$:

$$p_{\mathrm{p}} = W_{\mathrm{in1}} + W_{\mathrm{in2}} - W_{\mathrm{ex1}} - W_{\mathrm{ex3}} - W_{\mathrm{ex4}} \tag{12}$$

Relatively, it is straightforward to optimize Eq. (12) with a linear programming technique. In combination with the velocity field, the FEUB model for performing a dynamic analysis of passive earth pressure is expressed as

$$\underset{t,t\in[t_{\mathrm{start}},t_{\mathrm{end}}]}{\text{minimize}}\left\{\underset{\boldsymbol{X}_1,\boldsymbol{X}_2,\boldsymbol{X}_3}{\text{minimize}}\left[p_{\mathrm{p}}(t) = \boldsymbol{C}_{\mathrm{in1}}\boldsymbol{X}_2 + \boldsymbol{C}_{\mathrm{in2}}\boldsymbol{X}_3 - \boldsymbol{C}_{\mathrm{ex1}}\boldsymbol{X}_1 - \boldsymbol{C}_{\mathrm{ex3}}\boldsymbol{X}_1 - \boldsymbol{C}_{\mathrm{ex4}}\boldsymbol{X}_1\right]\right\}$$

$$\text{s.t.}\begin{cases} \boldsymbol{A}_{11}\boldsymbol{X}_1 - \boldsymbol{A}_{12}\boldsymbol{X}_2 = \boldsymbol{0} \\ \boldsymbol{A}_{21}\boldsymbol{X}_1 - \boldsymbol{A}_{23}\boldsymbol{X}_3 = \boldsymbol{0} \\ \boldsymbol{A}_{31}\boldsymbol{X}_1 = \boldsymbol{B}_{31} \\ \boldsymbol{C}_{\mathrm{ex2}}\boldsymbol{X}_1 = 1.0 \\ \boldsymbol{X}_2 \geq \boldsymbol{0} \\ \boldsymbol{X}_3 \geq \boldsymbol{0} \end{cases} \tag{13}$$

where $\boldsymbol{C}_{\mathrm{in1}}, \boldsymbol{C}_{\mathrm{in2}}, \boldsymbol{C}_{\mathrm{ex1}}, \boldsymbol{C}_{\mathrm{ex2}}, \boldsymbol{C}_{\mathrm{ex3}}, \boldsymbol{C}_{\mathrm{ex4}}$ are the vectors of objective function coefficients which are partially assembled from $\boldsymbol{C}^{\mathrm{e}}_{\mathrm{in1}}, \boldsymbol{C}^{\mathrm{d}}_{\mathrm{in2}}, \boldsymbol{C}^{\mathrm{e}}_{\mathrm{ex1}}, \boldsymbol{C}^{\mathrm{p}}_{\mathrm{ex2}}, \boldsymbol{C}^{\mathrm{e}}_{\mathrm{ex3}}$ and $\boldsymbol{C}^{c_{\mathrm{w}}}_{\mathrm{ex4}}$, respectively. The expressions of former three parameters can be found in Zhou and Qin (2020). $\boldsymbol{C}^{\mathrm{p}}_{\mathrm{ex2}}, \boldsymbol{C}^{\mathrm{e}}_{\mathrm{ex3}}$ and $\boldsymbol{C}^{c_{\mathrm{w}}}_{\mathrm{ex4}}$ are expressed as

$$\begin{cases} \boldsymbol{C}_{ex2}^{p} = \left[\eta_{px1}\eta_{py1}\eta_{px2}\eta_{py2}\right] \\ \boldsymbol{C}_{ex3}^{e} = \dfrac{A^{e}\gamma}{3g}\left[a_h(t,y)a_v(t,y)a_h(t,y)a_v(t,y)a_h(t,y)a_v(t,y)\right] \\ \boldsymbol{C}_{ex4}^{c_w} = \left[P_{c_wx1}P_{c_wy1}P_{c_wx2}P_{c_wy2}\right] \end{cases} \tag{14}$$

where η_{px1}, η_{py1}, η_{px2}, η_{py2} are the equivalent nodal loading coefficient of node i ($i = 1, 2$) to lateral earth pressure along the wall, g is the gravitational acceleration, A^e is the area of triangle e, P_{c_wx1}, P_{c_wy1}, P_{c_wx2}, P_{c_wy2} are the equivalent nodal loading of node i ($i = 1, 2$) to wall cohesive forces (c_w) along the wall. Hereof, $\boldsymbol{C}_{ex3}^{e}$ ($\boldsymbol{C}_{ex3}$) is time-dependent for a dynamic analysis (such as pseudo-dynamic analysis in this study) and constant for a static analysis (such as pseudo-static analysis).

Employing the interior point algorithm, Eq. (13) can be optimized by virtue of MATLAB. Analogous to FELB analysis, the same definition of passive earth pressure coefficient, Eq. (5), is used after having calculated passive earth pressure, and in this case it gives an upper-bound solution.

4. Comparison and discussion

4.1. Comparison with published literature

In the preceding analyses, FELB and FEUB methods are introduced to assess passive earth pressures. An interior point algorithm implemented into MATLAB is then applied to optimize lower- and upper-bound models. In order to validate the robustness of proposed procedures, comparison with published literature is carried out, where both lower- and upper-bound solutions are verified. Comparison results are illustrated in Fig. 2 where P-s and P-d solutions are also calculated and compared in a cohesionless soil. Based on the given parameters in Fig. 2, it is found that in the absence of earthquakes ($k_h = 0$), the FELB solutions of K_P present minor discrepancies with other lower bounds obtained from Shiau et al. (2008) and Tang et al. (2014). More interestingly, the FEUB solutions of this study are superior to other upper bounds by Soubra (2000) and Shiau et al. (2008). Accordingly, the FEUB and FELB procedures are proved to be valid for the assessment of static passive earth pressures. Note that in the presence of an earthquake (e.g. $k_h = 0.2$), rigorous upper- and lower-bound solutions of K_P calculated for $\varphi = 20°$, 25° and 30° are in good agreement with Soubra (2000) and Tang et al. (2014), respectively, thereby substantiating the validity of FEUB and FELB procedures for pseudo-static analyses of K_P. Moreover, the discrepancies between comparison results (upper vs. upper, lower vs. lower, and upper vs. lower) become smaller, with the decrement of φ. Meanwhile, non-rigorous limit equilibrium solutions are also cited for the case of $\varphi = 30°$. It is seen that the P-d limit equilibrium results (Ghosh and Kolathayar, 2011) are quite close to P-d FEUB K_P. In contrast, the P-s limit equilibrium solutions (Kumar, 2001) are within the range of lower and upper bounds, which are close to FELB solutions at small wall friction (δ_w/φ ratio) and approaching to FEUB solutions at large δ_w/φ ratios. Based on the above comparison, it can be concluded that the dynamic procedures for FEUB and FELB analyses of passive earth pressures are substantiated.

In an upper-bound analysis, it is straightforward to plot the velocity field at limit state after having optimized an upper bound solution. Taking the pseudo-static analysis for example, the velocity fields at $k_h = 0$ and 0.2 are compared with others. For the case of cohesionless backfilling soils with a flat ground and smooth vertical retaining wall, there is a Rankine solution for passive earth

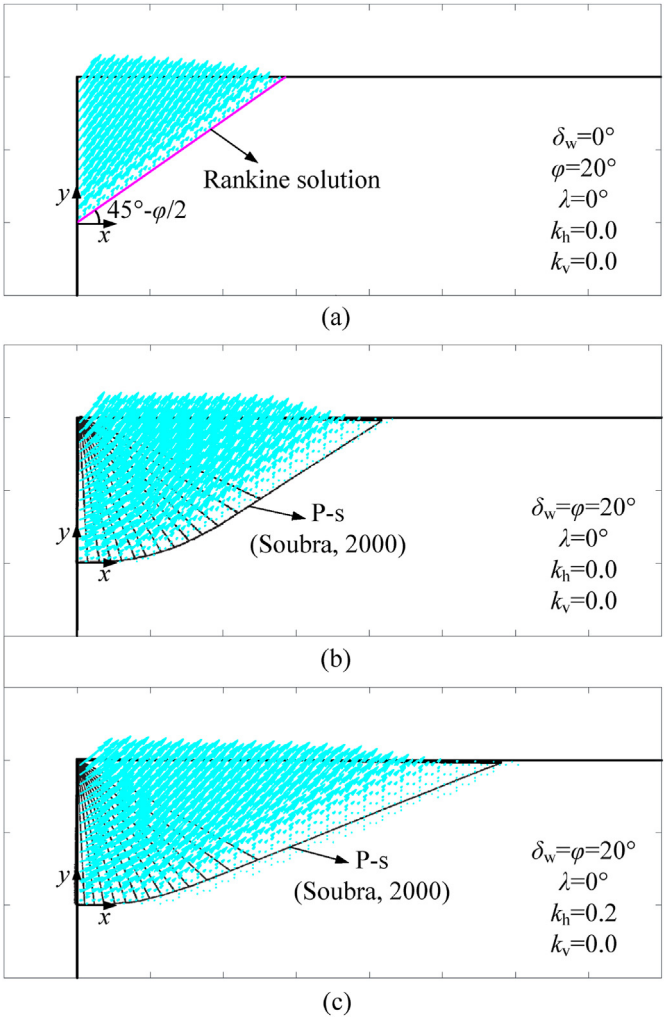

Fig. 3. Velocity fields of this study compared with the failure planes of: (a) static Rankine solution, (b) static solution in Soubra (2000) and (c) seismic solution in Soubra (2000).

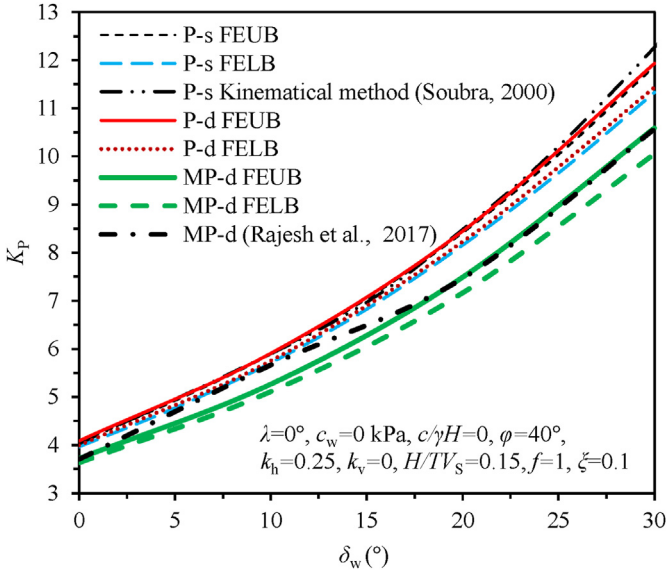

Fig. 4. Comparison of P-s, P-d and MP-d solutions of K_P from different approaches.

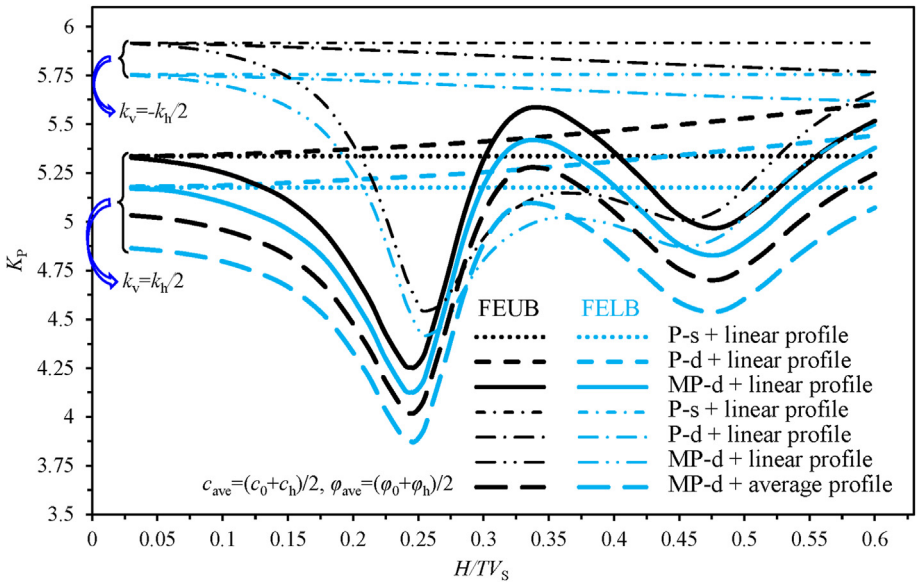

Fig. 5. Effects of dynamic properties on seismic K_P.

pressures where the failure plane is orientated at 45°-φ/2 to the horizontal plane, as shown in Fig. 3a. It is worthwhile pointing out that true solution of passive earth pressure is known for such simple example, and it equals Rankine (lower-bound) solution. When the critical velocity field from FEUB modelling is also plotted in this figure, it is found that such failure plane well encompasses the velocity field. This validates the FEUB result, and demonstrates the upper-bound solution is very much close to the lower-bound, as shown in Fig. 2, where the upper- and lower-bound solution almost merge. As for a rough wall, the Rankine solutions are not easily found. In this event, comparison is merely performed between upper-bound solutions in terms of velocity fields and failure planes, as presented in Fig. 3b and c. In Soubra (2000), the failure mechanism is comprised by several triangular rigid blocks, and at limit state the failure region is also similar to that encompassed by critical velocity fields, which verifies the FEUB procedure for passive earth pressure analyses.

Another comparison is made with considerations to MP-d analysis, with comparing results portrayed in Fig. 4. Similar as above, P-s FEUB solutions of K_P are again verified by Soubra (2000) with the kinematic method. Note that a smaller upper-bound solution is predicted from this study, which demonstrates a better estimate of K_P, particularly at higher δ_w values. If the original pseudo-dynamic approach is adopted for comparison, P-d FEUB and FELB solutions are increased slightly, in contrast to the P-s results. However, it shows that a significant decrement in K_P is resulted from the use of modified pseudo-dynamic approach. The decreased MP-d solutions of K_P is attributed to amplified seismic forces which facilitate soils to reach its passive limit state. With the use of same parameters and MP-d approach, the K_P solutions from limit equilibrium (Rajesh and Choudhury, 2017) are closer to FEUB results, especially at larger δ_w. On one hand, it indicates the robustness of the MP-d FEUB procedure for predicting seismic passive earth pressures. On the other hand, it reflects that limit equilibrium solutions are neither lower- or upper-bounds. Manifestly, an exponent increase in passive earth pressure coefficient is observed with increasing wall friction angles. This is because the presence of wall friction is to prevent backfilling soils moving upwards to reach its passive limit state, thereby requiring larger lateral forces to push soils at limit state. Interestingly, discrepancies between FEUB and FELB solutions gradually increase with increase of the angle δ_w, which demonstrates that such angle is quite sensitive and the selection of a proper δ_w has a significant effect on K_P.

4.2. Discussion on different earthquake inputs

In the following study, three types of earthquake inputs (seismic acceleration) are discussed, including P-s, P-d and MP-d. The solutions are obtained under the effects of wall parameters (H, λ, c_w, δ_w), soil properties (γ, c_0, c_h, φ_0, φ_h) and earthquake parameters (k_h, k_v, T, V_P, V_S, f, ξ), with the default input parameters: $H = 5$ m, $\lambda = 10°$, $c_w = 10$ kPa, $\delta_w = 20°$, $\gamma = 18$ kN/m^3, $c_0 = 25$ kPa, $c_h = 15$ kPa, $\varphi_0 = 30°$, $\varphi_h = 25°$, $k_h = 0.15$, $k_V = 0.5k_h$, $H/TV_S = 0.25$, $V_P = 1.87V_S$, $f = 1$, $\xi = 0.15$.

Its separate effects on passive earth pressure coefficient are investigated and compared as presented in Fig. 5, where the dynamic properties of earthquake and linearly varied MC strength parameters are considered. Hereof, H/TV_S ratios vary from 0.03 to 0.6, which could cover a quite large range of seismic examples (e.g. frequency of 0.6–12 Hz, for the case of $H = 5$ m and $V_S = 100$ m/s). For ease of distinction, positive acceleration is defined as rightwards and upwards. Undoubtedly, K_P in the P-s results remain unchanged under H/TV_S, due to the use of constant seismic coefficients. In contrast, P-d solutions of K_P show an upward trend with the increase of H/TV_S, for the case of $k_v = 0.5k_h$, which are no less than P-s results. This demonstrates that the optimal case appears when the vertical seismic forces act downwards and the downward force inhibits backfilling soils to reach its passive limit state, thereby requiring larger lateral thrust. However, for the case of $k_v = -0.5k_h$, an opposite outcome is produced, i.e. the K_P values in the P-d gradually decrease with increasing H/TV_S and are ought to be less than P-s K_P in this aspect. It is stemmed from the timing to reach an optimal passive limit state, which is influenced by the combined effects of H/TV_S and direction of vertical seismic forces. Given a duration of P-d earthquake, an increasing H/TV_S ratio tends to invert the direction of vertical seismic forces in the optimization of K_P, in contrast to P-s cases. However, owing to the introduction of MP-d approach where complicated expressions are derived to represent seismic accelerations, K_P results are nonlinearly affected by its dynamic properties. Specifically, MP-d K_P experiences a

significant decrement, followed by an upward trend, and then decreases and increases repeatedly, when H/TV_S increases. This is mainly attributed to the cyclic properties of MP-d seismic accelerations. More importantly, the minimal K_P values are sought at certain scenarios, which could push backfills soils to reach its passive limit state. Such minimal values are resulted from the 'resonance' effects when earthquake frequencies equal the natural frequencies of soils, particularly the fundamental soil frequency at $H/TV_S = 0.25$. Meanwhile, these results are highly associated with soil damping which aids to attenuate acceleration amplification. The case of $H/TV_S = 0.25$ demonstrates a worst case in passive earth pressure analyses and is hence adopted in the following calculations. Interestingly, it is found that the minimal K_P appears at different H/TV_S for the cases of $k_v = \pm 0.5k_h$. The main difference herein lies in the initial direction of vertical acceleration, which demonstrates an initial phase angle difference. Accordingly, phase angle plays an important roil in the magnitude of K_P and timing to reach its limit state. Overall, a passive state is easily to be achieved when the vertical seismic forces act upwards, with less lateral thrust required to push backfills soils, indicating a most dangerous scenario for the occurrence of passive failure. Meanwhile, MP-d K_P results are also calculated from average soil cohesion and friction angle, besides linearly varied profiles. It is observed that K_P shows an exactly same trend as that of using linearly MC parameters, with the increase in H/TV_S. Nonetheless, a much less K_P is induced when average MC strength parameters are assumed to represent linearly profiles, which will be further discussed later.

Note that in FEUB modelling, the velocity fields and failure planes can be readily obtained through post-processing. Effects of the P-s, P-d and MP-d seismic accelerations are therefore discussed with the above parameters when MC strength parameters are assumed to linear profiles and $k_v = 0.5k_h$, as portrayed in Fig. 6. At the worst case for MP-d analyses, i.e. $H/TV_S = 0.25$, it is found that passive failure blocks induced by the P-s and P-d accelerations are similar in shape and dimension, and in such case the increased P-d K_P value is resultant from downward seismic forces. However, a much larger failure block is produced to reach the passive limit state in the MP-d analysis, because the 'resonance' effects maximally amplify seismic accelerations. Meanwhile, another case with $H/TV_S = 0.5$ is also discussed and the required failure block becomes much smaller in contrast to the case of $H/TV_S = 0.25$. Although the earthquake frequency is approaching to second-order natural frequency of soils herein, amplification of seismic accelerations is attenuated by soil damping, and hence fewer lateral forces

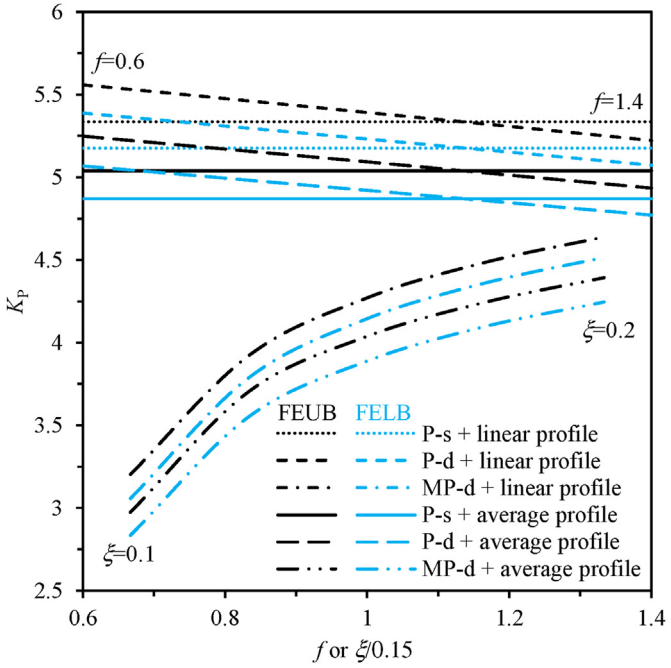

Fig. 7. Effects of soil amplification factor f and soil damping ξ on seismic K_P.

produced from earthquakes are provided and more other lateral forces are required to push backfill soils to reach its limit state. It is likely that the critical failure plane is composed by a curved section near the wall and a straight line far away from the wall.

As discussed above, the P-s, P-d and MP-d approaches are adopted to represent seismic accelerations. It is noted that soil amplification factor f is used to directly portray linearly amplified acceleration profiles when the shear waves propagate upwards. In contrast, seismic accelerations amplify nonlinearly in the MP-d approach, and the amplification is restrained by soil damping ξ. Fig. 7 presents the effects of these two parameters on seismic K_P where f varies from 0.6 to 1.4 and ξ changes from 0.1 to 0.2 (normalized by 0.15 in this figure), based on the parameters used in Fig. 5. As expected, the K_P value in the P-s solutions is irrespective of factors f and ξ, which are not included in constant seismic accelerations. It is observed that a linear decrement in K_P is induced by an increase of f. A large f means increased acceleration and seismic

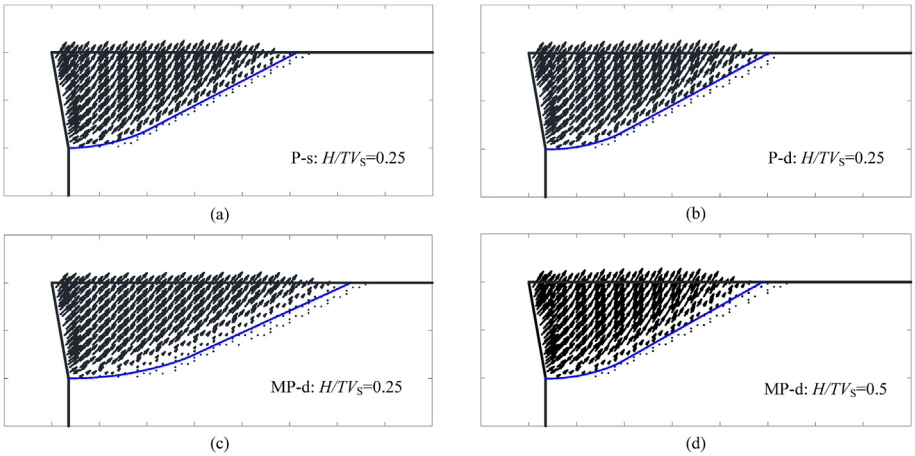

Fig. 6. Velocity fields and failure planes from: (a) P-s analysis with $H/TV_S = 0.25$, (b) P-d analysis with $H/TV_S = 0.25$, (c) MP-d analysis with $H/TV_S = 0.25$, and (d) MP-d analysis with $H/TV_S = 0.5$.

forces to push soils rightwards, thereby requiring less lateral thrust and passive earth pressures in turn. In this way, selection of a proper factor f can produce an equivalent K_P as that of P-s approach. As for MP-d analyses, due to the soil damping, the FEUB and FELB solutions of K_P are significantly increased with increasing ξ. The larger ξ, the less seismic forces, and the more lateral forces required to push backfilling soils. Since the worst scenario (at $H/TV_S = 0.25$) is discussed herein, the amplified seismic acceleration is still larger than those of P-s and P-d inputs, the K_P value is hence smaller. Less than 5% difference between FEUB and FELB solutions demonstrates a quite reliable prediction of true passive earth pressure (K_P).

5. FEUB and FELB solutions

Following the preceding FEUB and FELB procedures, the P-s, P-d and MP-d solutions of passive earth pressure coefficients are calculated. In this section, some influence factors such as wall inclination angle (λ), wall friction angle (δ_w), wall cohesion (c_w), and linearly increased MC soil strength parameters are discussed, aiming to provide a better understanding of their effects on a rigid retaining wall at limit state. These results are presented in terms of dimensionless coefficient K_P, for the ease of practical use in the design or assessment of retaining wall problems.

Fig. 8 illustrates the effects of wall inclination on the P-s, P-d and MP-d solutions of K_P, considering linearly varied and constant (average) MC strength profiles. Manifestly, K_P decreases significantly with the increase of angle λ, demonstrating that passive failure is more likely to happen at large and positive λ values. Note that in site where an arch bridge is to be designed or constructed, it is fortunate to find that the λ value as defined in Fig. 1 is usually negative, and hence a much larger lateral force is required to make surrounding soils reach its passive limit state. In other words, such topography tends to have a large capacity to resist the thrust force transferred from the abutment. Similar as above, P-d K_P at $k_v = 0.5k_h$ is a little bit greater than P-s solutions because the optimal P-d solution is sought when vertical seismic forces act downwards. Reversely, the MP-d FEUB and FELB solutions are much less than the above, owing to amplified seismic forces which facilitate to push soils upwards. For the case of backfilling soils with a linearly varied MC strength profile, the use of average strength

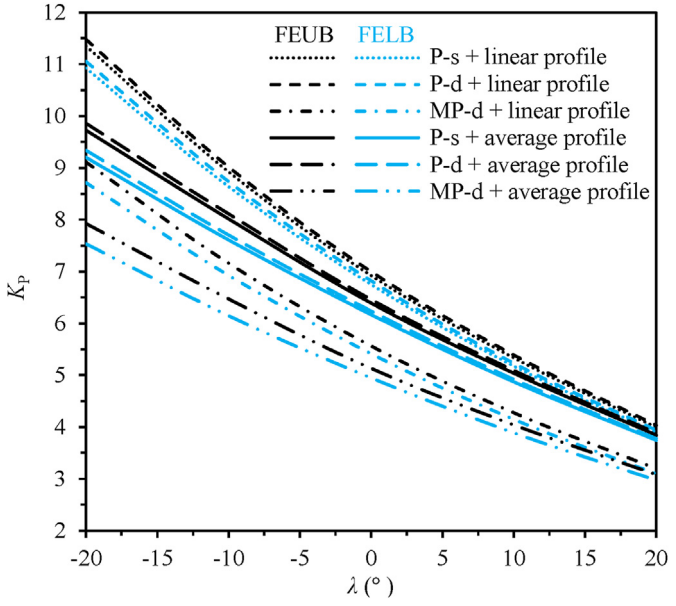

Fig. 8. Influence of wall inclination angle on seismic K_P.

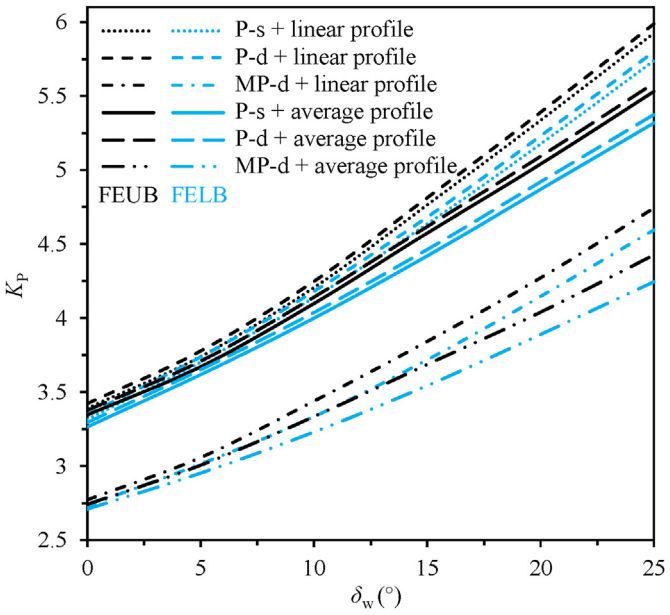

Fig. 9. Influence of wall friction angle on seismic K_P.

parameters tends to apparently under-estimate passive earth pressures, based on which the design of such retaining wall would be not economical. Therefore, in an effort to well predict solutions of seismic K_P, adoption of meaningful parameters is a prerequisite, such as reliable soil parameters and MP-d acceleration inputs with more detailed dynamic information.

In Rankine method, a smooth wall is assumed, and wall friction effects cannot be accounted for. Resorting to powerful FEUB and FELB procedures, non-zero wall friction can be readily considered, and its effect on seismic passive earth pressure coefficients is illustrated in Fig. 9. It is expected that an increase in wall friction angle tends to produce a large K_P value. Since the presence of wall friction is to prevent nearby soils moving upwards, it inhibits soils to reach its passive limit state, and additional lateral force is therefore required. Again, it is substantiated that the P-d solutions are slightly greater than P-s results, and the use of average MC strength parameters could under-estimate K_P results. In contrast, MP-d K_P is roughly 20% lower than the pseudo-static in the presence of large wall friction. More importantly, both FEUB and FELB solutions are computed. It is observed that the discrepancies between upper- and lower-bound solutions gradually augment with increase of the wall friction. However, less than 4.2% difference is induced, demonstrating a sound estimate of true passive earth pressure coefficient because it is well within this small range. A more accurate K_P is estimated if a rigid retaining wall is not that rough, and this is substantiated by a nearly true solution obtained for a smooth wall in Fig. 2.

Velocity fields and failure planes under the effects of wall inclination and friction angles are shown in Fig. 10 where MC strength parameters are assumed to linear profiles in the MP-d analyses. Similar to that in Fig. 3a, the critical failure plane is likely to be a straight line for a smooth wall, although such wall is inclined at 10° outwards. Note that with the increase of angle δ_w, the passive failure block becomes larger, thereby requiring greater lateral force (also K_P) to push soils behind a retaining wall to reach its passive limit state, as shown in Fig. 9. Meanwhile, the failure plane near wall toe gradually becomes curved. If a rigid retaining wall is designed with a negative λ value (e.g. −10°), the area encompassed by velocity fields continues to increase, in contrast to

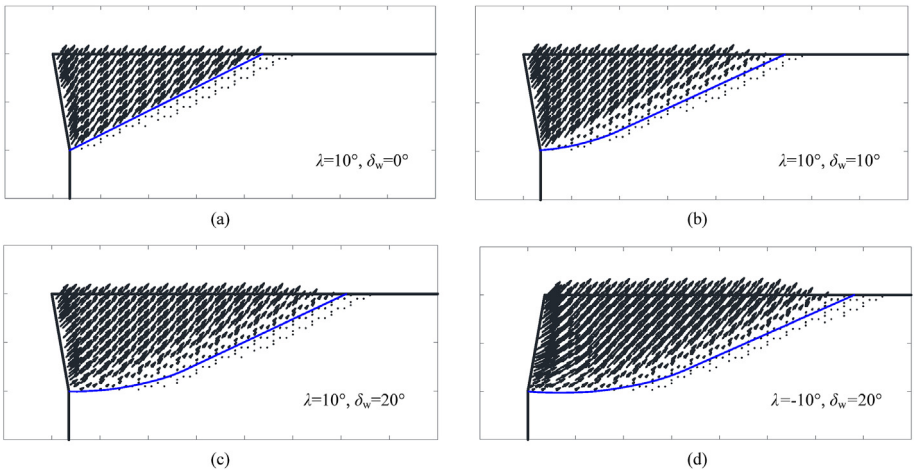

Fig. 10. Velocity fields and failure planes under different λ and δ_w values: (a) $\lambda = 10°$, $\delta_w = 0°$, (b) $\lambda = 10°$, $\delta_w = 10°$, (c) $\lambda = 10°$, $\delta_w = 20°$, and (d) $\lambda = -10°$, $\delta_w = 20°$.

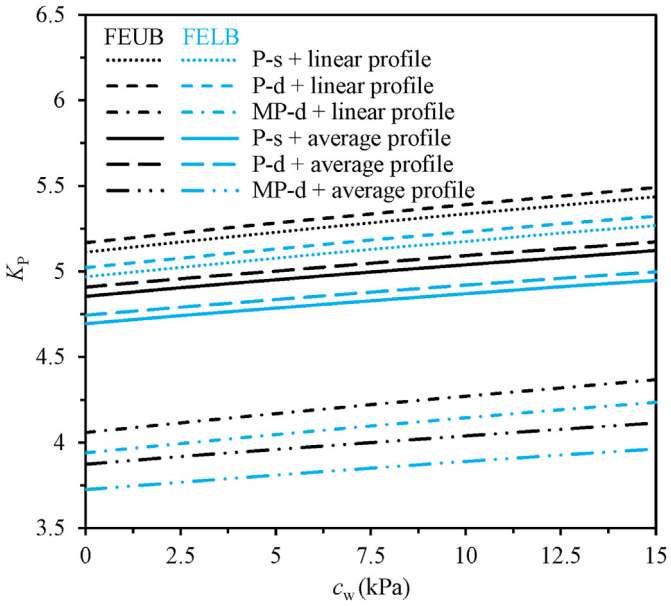

Fig. 11. Influence of wall cohesion on seismic K_P.

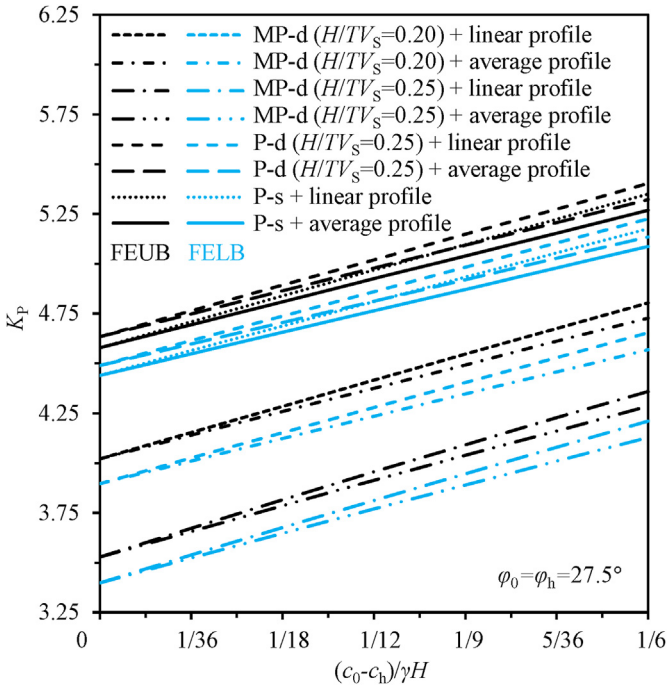

Fig. 12. Influence of soil cohesion increase on P-s, P-d and MP-d solutions of K_P.

that of $\lambda = 10°$. The same explanation can be used to interpret the change pattern of seismic K_P in Fig. 8. Overall, it shows that soils behind a rigid retaining wall show a rotational-translational failure mode, from the perspective of velocity fields.

Apart from wall friction, wall cohesion is another parameter influencing seismic passive earth pressure on a retaining wall, and its effect is presented in Fig. 11. Similar to wall friction's effect, an increasing K_P is produced with an increment of wall cohesion, and differently, its increasing trend tends to be linear, which is attributed to a linear contribution of wall cohesion's effect to total external rates of work and can be found in Eq. (10). As expected, the largest K_P is yielded with the use of P-d approach, followed by P-s one, and a much less K_P is obtained by MP-d approach. This depends on the magnitude of seismic forces, which facilitates the backfilling soils to reach a passive limit state. The lager seismic forces to push soils from the MP-d analysis, the smaller thrust force from the retaining wall required. Based on different outcomes produced by those three seismic inputs, it is preferred to adopting the seismic acceleration closer to that in practice, so as to yield more reliable results. Again, it displays that the use of average MC parameters would under-estimate seismic passive earth pressure coefficient, in comparison with a linearly increased profile for soil cohesion and friction angle.

It is not unusual that soil cohesion tends to present a linearly increased profile along depth in backfilling soils with varied degrees of compaction. Adoption of FEUB and FELB method could readily take these effects into consideration, and the results are shown in Fig. 12. Hereof, soil cohesion at ground surface is fixed as $c_h = 15$ kPa, and varying c_0 values are in the range of 15–30 kPa. Apart from a linear increase in soil cohesion, an average profile specific to arithmetic mean of c_h and c_0 is considered as a special case which is widely adopted in conventional limit analysis. Manifestly, K_P tends to increase linearly with the increase of soil cohesion increment, regardless of differing earthquake inputs and FEUB or FELB methods. Overall, the use of average profile produces

smaller K_P values, in contrast to the linear profile, and the discrepancy becomes gradually widened. It also shows that adoption of MP-d approach yields a much lower K_P, when comparing with P-s and P-d solutions. The reduced K_P is highly dependent on H/TV_S ratios which play an important role in the amplification of seismic forces. As stated earlier at $H/TV_S = 0.25$, resonance effects occur, and seismic forces are amplified to the highest level, providing the maximum driving force to push backfilling soils to reach its passive limit state, thereby requiring least lateral forces with smallest K_P in turn. Aiming to design a conservative and economical retaining wall, it is of vital engineering significance to have a reliable soil strength profile and a proper manner to consider external loadings such as seismic forces.

Apart from varied soil cohesion, internal friction angle of soils may also vary with depth, due to geological formation process. At fixed soil friction angle at ground surface (e.g. $\varphi_h = 25°$), Fig. 13 presents the effects of soil friction angle at the bottom (φ_0) on passive earth pressure coefficients. As expected the FEUB and FELB solutions of K_P experience an upward trend when φ_0 is increased from 20° to 30°. An increased K_P value is attributed to additional resistance provided by soils behind a wall to resist its upward movement, which in turn requires more lateral force to push soils to reach passive limit state. For example, K_P at $\varphi_0 = 30°$ is 34.5%–41.2% (depending on the adoption of different seismic inputs) higher than that at $\varphi_0 = 20°$. This demonstrates that soil friction angle has a substantial effect on the determination of K_P. If an average soil friction angle φ is assumed to represent such linear profile, it is observed that at $\varphi_0\,(\varphi) = 25°$ the same solution is obtained. However, K_P on the left side of this point is greater for the case of using constant profiles, and vice versa. In other words, the use of assumed constant soil friction angle without considering its true profile may over-estimate or under-estimate K_P solutions. In contrast to the P-s and P-d solutions with $f = 1.0$, the MP-d solutions are much lower and highly dependent upon H/TV_S ratios. As for above results, the discrepancy between FEUB and FELB solutions is as low as 4.2%, based on which true K_P value is well estimated.

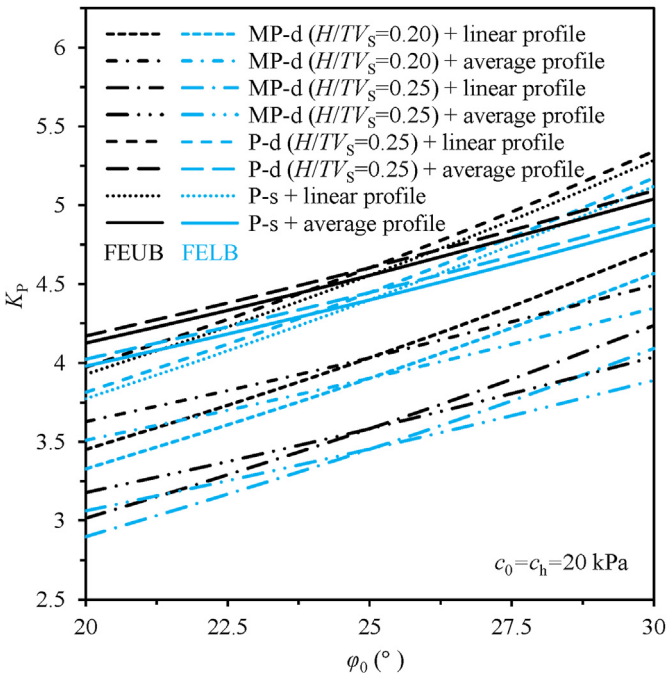

Fig. 13. Influence of soil friction angle φ_0 on P-s, P-d and MP-d solutions of K_P.

6. Conclusions

This study aims to predict seismic passive earth pressure (coefficient) acting on a rigid retaining wall based on plasticity theory. Pseudo-static, original and modified pseudo-dynamic approaches are adopted to represent seismic acceleration inputs. In order to account for linearly varied MC soil strength profiles in the process of generating a kinematically admissible velocity field and a statically allowable stress field, the finite element method is adopted to discretize the domain of interest into finite elements.

(1) Based on discretized feasible velocity and stress fields, stress equilibrium and work rate equations are constructed, and specific upper- and lower-bound solutions are obtained with an interior point algorithm, forming the FEUB and FELB procedures. Combining the merits of limit analysis with finite element method, the proposed FEUB and FELB procedures are powerful to consider complicated scenarios which cannot be readily solved in conventional upper- and lower-bound analyses. After having validated the robustness of the proposed FEUB and FELB procedures with published literature, the effects of influence factors such as wall inclination and friction angle, earthquake inputs and MC strength properties on K_P are investigated.

(2) At passive limit state, the required lateral force is increased with increments in wall friction angle, soil damping ratio and MC strength parameters, and with a decrement of wall inclination angle and soil amplification factor, thereby producing an increased K_P. It shows that a more reliable prediction of seismic passive earth pressure coefficient can be obtained by virtue of modified pseudo-dynamic approach where more dynamic properties of an earthquake are accounted for and with the use of a closer to actual MC soil strength profiles.

(3) Owing to amplified seismic acceleration, the FEUB and FELB solutions of K_P are significantly reduced, which tends to indicate a more dangerous scenario. The use of constant MC strength parameters to represent linearly varied profiles would over-estimate or under-estimate seismic K_P. Another finding of this study is that less than 5% difference between the FEUB and FELB solutions of seismic K_P is obtained, and such narrowed range of upper and lower bounds aids to provide a reliable and meaningful estimate for true passive earth pressures.

Data availability statement

The data from the present study are available by the corresponding author after reasonable request.

Declaration of competing interest

The authors declare that they have no known competing financial interests or personal relationships that could have appeared to influence the work reported in this paper.

Acknowledgements

The research was financially supported by National Natural Science Foundation of China (Grant Nos. 52108302 and 52009046), Fundamental Research Funds for the Central Universities of Huaqiao University (Grant No. ZQN-914).

References

Chen, W.F., 1975. Limit Analysis and Soil Plasticity. Elsevier, Amsterdam, the Netherlands.

Chen, W.F., Liu, X.L., 1990. Limit Analysis in Soil Mechanics. Elsevier, Amsterdam, the Netherlands.

Choudhury, D., Nimbalkar, S., 2005. Seismic passive resistance by pseudo-dynamic method. Geotechnique 55 (9), 699–702.

Fathipour, H., Payan, M., Chenari, R.J., Senetakis, K., 2021. Lower bound analysis of modified pseudo-dynamic lateral earth pressures for retaining wall-backfill system with depth-varying damping using FEM-Second order cone programming. Int. J. Numer. Anal. Methods GeoMech. 45 (16), 2371–2387.

Fathipour, H., Siahmazgi, A.S., Payan, M., Chenari, R.J., 2020. Evaluation of the lateral earth pressure in unsaturated soils with finite element limit analysis using second-order cone programming. Comput. Geotech. 125, 103587.

Ghosh, P., Kolathayar, S., 2011. Seismic passive earth pressure behind non- vertical wall with composite failure mechanism: pseudo-dynamic approach. Geotech. Geol. Eng. 29 (3), 363–373.

Kumar, J., 2001. Seismic passive earth pressure coefficients for sands. Can. Geotech. J. 38 (4), 876–881.

Lancellotta, R., 2007. Lower-bound approach for seismic passive earth resistance. Geotechnique 57 (3), 319–321.

Li, Z.W., Li, T.Z., Yang, X.L., 2020. Three-dimensional active earth pressure from cohesive backfills with tensile strength cutoff. Int. J. Numer. Anal. Methods GeoMech. 44 (7), 942–961.

Li, Z.W., Yang, X.L., 2019a. Active earth pressure for retaining structures in cohesive backfills with tensile strength cut-off. Comput. Geotech. 110, 242–250.

Li, Z.W., Yang, X.L., 2019b. Active earth pressure from unsaturated soils with different water levels. Int. J. GeoMech. 19 (7), 06019013.

Liu, S.Y., Xia, Y., Liang, L., 2018. A modified logarithmic spiral method for determining passive earth pressure. J. Rock Mech. Geotech. Eng. 10 (6), 1171–1182.

Nimbalkar, S., Choudhury, D., 2007. Sliding stability and seismic design of retaining wall by pseudo-dynamic method for passive case. Soil Dynam. Earthq. Eng. 27 (6), 497–505.

Oberhollenzer, S., Tschuchnigg, F., Schweiger, H.F., 2018. Finite element analyses of slope stability problems using non-associated plasticity. J. Rock Mech. Geotech. Eng. 10 (6), 1091–1101.

Pain, A., Choudhury, D., Bhattacharyya, S.K., 2017. Seismic rotational stability of gravity retaining walls by modified pseudo-dynamic method. Soil Dynam. Earthq. Eng. 94, 244–253.

Qin, C.B., Chian, S.C., 2018. Kinematic analysis of seismic slope stability with a discretisation technique and pseudo-dynamic approach: a new perspective. Geotechnique 68 (6), 492–503.

Qin, C.B., Chian, S.C., 2019. Pseudo-static/dynamic solutions of required reinforcement force for steep slopes using discretization-based kinematic analysis. J. Rock Mech. Geotech. Eng. 11 (2), 289–299.

Qin, C.B., Chian, S.C., 2020. Pseudo-dynamic lateral earth pressures on rigid walls with varying cohesive-frictional backfill. Comput. Geotech. 119, 103289.

Qin, C.B., Zhou, J.F., 2023. On the seismic stability of soil slopes containing dual weak layers: true failure load assessment by finite-element limit-analysis. Acta Geotechnica 1–23.

Rajesh, B.G., Choudhury, D., 2017. Seismic passive earth resistance in submerged soils using modified pseudo-dynamic method with curved rupture surface. Mar. Georesour. Geotechnol. 35 (7), 930–938.

Santhoshkumar, G., Ghosh, P., 2020. Seismic stability of a broken-back retaining wall using adaptive collapse mechanism. Int. J. GeoMech. 20 (9), 04020154.

Shiau, J.S., Augarde, C.E., Lyamin, A.V., Sloan, S.W., 2008. Finite element limit analysis of passive earth resistance in cohesionless soils. Soils Found. 48 (6), 843–850.

Soubra, A.H., 2000. Static and seismic passive earth pressure coefficients on rigid retaining structures. Can. Geotech. J. 37 (2), 463–478.

Srikar, G., Mittal, S., 2020. Seismic analysis of retaining wall subjected to surcharge: a modified pseudodynamic approach. Int. J. GeoMech. 20 (9), 06020022.

Steedman, R.S., Zeng, X., 1990. The influence of phase on the calculation of pseudo-static earth pressure on a retaining wall. Geotechnique 40 (1), 103–112.

Tang, C., Phoon, K.K., Toh, K.C., 2014. Lower-bound limit analysis of seismic passive earth pressure on rigid walls. Int. J. GeoMech. 14 (5), 04014022.

Ukritchon, B., Keawsawasvong, S., 2018. A new design equation for drained stability of conical slopes in cohesive-frictional soils. J. Rock Mech. Geotech. Eng. 10 (2), 358–366.

Yang, X.L., Li, Z.W., 2018. Kinematical analysis of 3D passive earth pressure with nonlinear yield criterion. Int. J. Numer. Anal. Methods GeoMech. 42 (7), 916–930.

Zhou, J.F., Qin, C.B., 2020. Finite-element upper-bound analysis of seismic slope stability considering pseudo-dynamic approach. Comput. Geotech. 122, 103530.

Zhou, J.F., Qin, C.B., 2022. Stability analysis of unsaturated soil slopes under reservoir drawdown and rainfall conditions: steady and transient state analysis. Comput. Geotech. 142, 104541.

Zhou, J.F., Qin, C.B., 2023. Influence of soft band on seismic slope stability by finite-element limit-analysis modelling. Comput. Geotech. 158, 105396.

Changbing Qin received his BEng degree from Zhengzhou University in 2012, MEng degree from Central South University in 2015, and PhD degree from National University of Singapore in 2019. He is currently working as a Professor at the Chongqing University. His research interest includes (1) Slope engineering mainly on stability analyses, landslides, and debris flow, and (2) Tunnel engineering mainly on tunnel roof and face analyses.